INTERNATIONAL JOURNAL OF HYDROGEN ENERGY 37 (2012) 14624–14631

Available online at www.sciencedirect.com

SciVerse ScienceDirect

journal homepage: www.elsevier.com/locate/he

Effect of syngas addition on performance of a spark-ignited gasoline engine at lean conditions

Xiaoxu Dai, Changwei Ji, Shuofeng Wang, Chen Liang, Xiaolong Liu, Bingjie Ju*

College of Environmental and Energy Engineering, Beijing University of Technology, Beijing 100124, China

ARTICLE INFO

Article history:
Received 23 May 2012
Received in revised form
9 July 2012
Accepted 10 July 2012
Available online 9 August 2012

Keywords:
Syngas
Steam reforming
Exhaust heat recovery
Emissions
Lean combustion
SI engines

ABSTRACT

The paper studied the effect of syngas addition on performance of a gasoline engine at lean conditions. The engine ran at 1800 rpm and a manifolds absolute pressure of 61.5 kPa. The spark timing for the maximum brake torque was adopted for each testing point. The syngas volume fraction in the total intake gas was fixed at 0% and 2.5%. The test results showed that peak cylinder pressure and indicated thermal efficiency were enhanced after the syngas enrichment. Flame development and propagation durations of the 2.5% syngas-blended engine were reduced by 7.2 and 5.7 °CA, compared with those of the original engine at an excess air ratio of 1.36. The coefficient of variation in the indicated mean effective pressure showed a noticeable decrease after the syngas addition. CO and NOx emissions were slightly increased with the syngas enrichment. HC emissions were first reduced and then increased after the syngas blending.

1. Introduction

Concerning the limited energy reserves and adversely increased environmental pollution, improving the internal combustion (IC) engine efficiency and emissions performance has pushed researchers to find new alternative fuels. Compared with gasoline, hydrogen and carbon monoxide have many notable positive physicochemical and combustion properties. Therefore, the syngas is a good alternative fuel which can be applied on vehicles [1–15]. However, because the energy densities of hydrogen and carbon monoxide on volume basis are much lower than that of gasoline, the syngas-fueled engines are prone to produce less power than gasoline engines [16,17].

The syngas which was introduced into gasoline engines can take the positive properties of syngas and fossil fuels [2,18–21]. Huang et al. [22] investigated the effect of exhaust gas recirculation and hydrogen addition on combustion and emissions performance of a spark ignition (SI) natural gas engine. The test results showed that the hydrogen addition could improve the engine combustion stability and increase the engine power. Andrea et al. [23] conducted an experiment to study the performance of a two-cylinder carburetor gasoline engine enriched by hydrogen. He found that hydrogen could obviously improve the engine performance when the overall equivalence ratio was lower than 0.85. Ji et al. [24–26] studied the effect of hydrogen addition on the engine combustion and emissions characteristics. According to the test results, the engine thermal efficiency and emissions performance were improved with the increase of hydrogen addition level. Meanwhile, flame development and propagation durations were shortened with the hydrogen enrichment at lean conditions. Shudo [27] studied a homogeneous charge compression ignition (HCCI) engine fueled by on-board

* *Corresponding author*. Tel./fax: +86 1067392126.
E-mail address: chwji@bjut.edu.cn (C. Ji).

http://dx.doi.org/10.1016/j.ijhydene.2012.07.039

reformed gases of methanol with waste heat recovery. He got the conclusion that the dimethyl ether (DME) and methanol-reformed gas (MRG) could increase engine thermal efficiency. Besides, hydrogen was an effective ignition controller for the HCCI engines fueled with DME.

Although the syngas addition could improve the engine combustion and emissions performance, the risks in syngas storage and transport are still barriers for the commercialization of syngas-blended engines. Comparatively, producing syngas by fuel reforming with the exhaust heat recovery is a feasible strategy [28]. Due to the high hydrogen yield and low rate of by-products, the steam reforming of ethanol (SRE) is a reliable method to produce syngas. And the syngas could be used to improve the engine overall efficiency and performance [29]. Ethanol is a renewable material with many positive properties. For example, it is biodegradable and convenient for transportation [30]. Ethanol steam reforming for producing hydrogen over $Co/MgAl_2O_4$ catalysts promoted by noble metals was studied by Profeti et al. [31]. The test results showed that the performance of $Co/MgAl_2O_4$ was boosted by adding small amounts of noble metals (Pt, Ru, Ir). Park et al. [32] investigated the performance of an SI engine fueled with the gasoline and ethanol–syngas. He found that the combustion stability was enhanced after the addition of simulated syngas. Moreover, the simulated syngas could also reduce HC and NOx emissions.

Although there are many publications that have researched the effect of hydrogen addition on the engine performance, few studies have focused on the effect of syngas addition on the performance of an SI engine with exhaust heat recovery. In this paper, the effect of syngas addition on the combustion and emissions characteristics of a gasoline engine at lean conditions was investigated. A self-designed fuel reforming reactor with the copper-based catalysts was connected to the engine tailpipe. The feedstocks of SRE could be converted into the syngas when the catalysts were heated by the exhaust gas. The engine was run at a constant engine speed of 1800 rpm and a manifolds absolute pressure (MAP) of 61.5 kPa with two syngas volume fractions of 0% and 2.5% in the total intake gas, respectively. Additionally, excess air ratio was increased from 1.01 to 1.36 by adjusting the injection duration of gasoline.

2. Experimental setup and procedure

2.1. *Experimental setup*

2.1.1. *Catalyst preparation*

Copper and nickel show better performance in SRE for hydrogen production than others. Also, compared with the noble metal catalysts, the comparatively low cost of copper and nickel make them more promising for application. In this study, the copper based catalysts are coated to the ceramic spherical body. The γ-Al_2O_3 carrier is obtained by impregnating α·Al_2O_3·nH_2O, $Ba(NO_3)_2$, $La(NO_3)_3$·$6H_2O$ and $Ce(NO_3)_3$·$6H_2O$ with an aqueous deionized water which is constantly being vigorously stirred, followed by exsiccation at 110 °C for 24 h and calcinations at 500 °C for 4 h. The copper based catalyst sample is prepared by impregnating a γ-Al_2O_3 carrier, with an aqueous solution of $Cu(NO_3)_2$·$3H_2O$, $Zn(NO_3)_2$·$6H_2O$, $Al(NO_3)_3$·$9H_2O$ and $Zr(NO_3)_4$·$5H_2O$, followed by exsiccation at 110 °C for 2 h and calcinations at 500 °C for 4 h.

2.1.2. *Engine testing system*

The schematic diagram of the experimental system is shown in Fig. 1. The test engine is a 1.6 L, four-cylinder, SI engine produced by Beijing Hyundai Motors, which has a rated power output of 82.32 kW at 6000 rpm and a rated torque of 143.28 N m at 4500 rpm. A hybrid electronic control unit (HECU) which communicates with the engine original electronic control unit (OECU) and a calibration computer is used to govern the engine spark timing, injection timing and duration of the gasoline. The syngas produced from SRE is directly introduced into the fourth cylinder of the engine. The SRE reactions are carried out on a self-designed fuel reforming reactor which recovers the exhaust heat. When the reactor is heated by the engine exhaust gases, the feedstocks of SRE are initially transformed from a liquid phase into a gaseous phase.

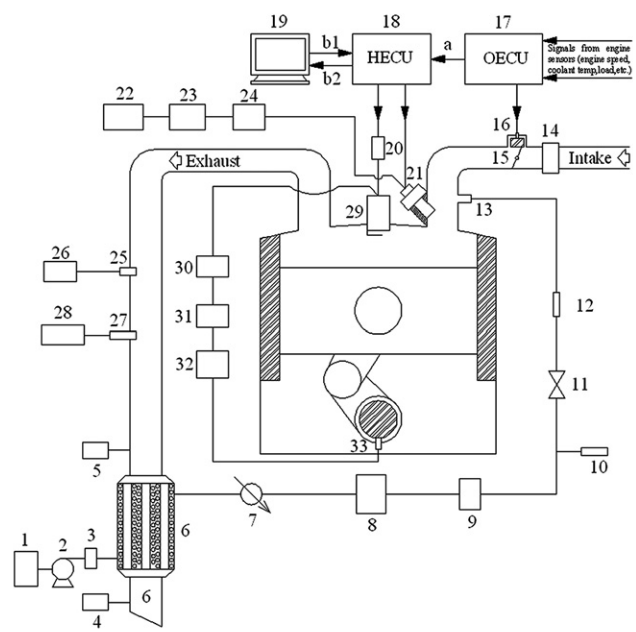

Fig. 1 – The schematics of the experiment system. 1. Feedstock tank; 2. Feedstock pump; 3. Feedstock flow meter; 4. Exhaust gas outtake temperature transducer; 5. Exhaust gas intake temperature transducer; 6. Reactor; 7. Cold-trap; 8. Pressure stabilizing vessel with desiccant; 9. Syngas flow meter; 10. Syngas sampling pipe; 11. Shutoff valve; 12. One-way valve; 13. Syngas intake pipe; 14. Air mass flow meter; 15. Throttle; 16. Idle valve; 17. Original ECU (OECU); 18. Hybrid electronic control unit ECU (HECU); 19. Calibration computer; 20. Ignition module; 21. Fuel injector; 22. Fuel tank; 23. Fuel mass flow meter; 24. Fuel pump; 25. O_2 sensor; 26. A/F analyzer; 27. Emissions sampling pipe; 28. MEXA-7100 emissions analyzer; 29. Pressure transducer with a spark plug; 30. Charge amplifier; 31. A/D converter; 32. Combustion analyzer; 33. Optical encoder; a. Signals from OECU to HECU; b1. Calibration and control signals from the calibration computer to HECU; b2. Data signals from HECU to a calibration PC.

Then, the gaseous feedstocks could be further converted into the syngas with the effect of catalysts. Two temperature transducers are placed on the anterior and posterior ends of the reactor to monitor the exhaust temperature. A pump and a flow rate controller are utilized to adjust the feedstock flow rate. A cold-trap and a pressure stabilizing vessel with desiccant are applied to purify the syngas. The syngas volume flow rate is monitored by a flow meter, and the syngas is sampled by a gas sampling pipe. A gas chromatograph (GC) is used to analyze the concentration of components in the sampled gas. A one-way valve is utilized to prevent refluxing of the syngas.

A GW 160 eddy current dynamometer is connected to the engine to control engine speed by automatically adjusting the load applied on the engine crankshaft (measurement deviation: $<\pm1$ rpm, $<\pm0.28$ N m in torque). The gasoline flow rate is determined by a FC2210 gasoline mass flow meter (measurement uncertainty: $<\pm0.4$ g/min). The air mass flow rate is monitored by a 20N060 thermal mass flow meter (measurement uncertainties: $<\pm0.1$ L/min). The in-cylinder pressure data acquisition and combustion analysis system consists of a Kistler 2613B optical encoder (crank angle resolution: 0.2 °CA, measurement deviation $<\pm0.01$ °CA), a Kistler 6117BCD17 cylinder pressure transducer with a spark plug (measurement uncertainty: $<\pm0.3$ bar) and a Dewetron combustion analyzer. The cylinder pressure transducer is screwed into the cylinder head of the fourth cylinder to acquire the combustion cylinder pressure and enforce ignition of the fourth cylinder. The cylinder pressure and relevant crank signals are sampled for over 200 consecutive cycles and treated via the DEWE-CA combustion analysis software. The exhaust emissions of NOx, HC and CO are measured by a Horiba MEXA-7100DEGR emissions analyzer and the measurement sensitivities for all emissions are 1 ppm. NOx are measured using the chemiluminescent method, HC emissions are determined by the hydrogen flame ionization detection method, and CO is detected by the nondispersive infrared method.

2.2. *Experimental procedure*

The experiment began when the engine was fully warmed up. During the test, the coolant and lubricant oil temperatures were kept between 85 ± 1 °C and 90 ± 1 °C. The engine speed was fixed at a constant 1800 rpm. The main throttle was adjusted to ensure that the MAP was kept at 61.5 kPa for all testing points. The HECU was used to control the injection timing and duration of gasoline through the OECU and a calibration computer. The spark timing for the maximum brake torque (MBT) was adopted for each testing point. The syngas volume fraction in the total intake gas (air and syngas) was fixed at 0% and 2.5%, respectively. The excess air ratio was gradually raised from 1.01 to 1.36 by reducing the gasoline injection duration. The syngas volume fraction (α) and the excess air ratio (λ) are defined as:

$$\alpha = \dot{\upsilon}_s/(\dot{\upsilon}_s + \dot{\upsilon}_{air}) \tag{1}$$

$$\lambda = \dot{m}_{air}/(\dot{m}_g \cdot AF_{st,g} + \dot{m}_{H_2} \cdot AF_{st,H_2} + \dot{m}_{CO} \cdot AF_{st,CO}) \tag{2}$$

In Eqs. (1) and (2), $\dot{\upsilon}_s$ and $\dot{\upsilon}_{air}$ are the measured volumetric flow rates of syngas and air at normal conditions (L/h), respectively; $\dot{m}_{air}$, $\dot{m}_g$, $\dot{m}_{H_2}$ and $\dot{m}_{Co}$ represent the measured air, gasoline, hydrogen and carbon monoxide mass flow rates (g/min); $AF_{st,g}$, AF_{st,H_2} and $AF_{st,CO}$ are the stoichiometric air-to-fuel ratios of gasoline, hydrogen and carbon monoxide ($AF_{st,g} = 14.6$ $AF_{st,H_2} = 34.3$ and $AF_{st,CO} = 2.5$).

During the test, the excess air ratio was monitored by a Horiba MEXA-110 A/F analyzer (measurement deviation: 0.1 A/F at A/F = 14.7). The H/C molar ratio setting on the instrument was adjusted according to the measured gasoline, hydrogen and carbon monoxide mass flow rates. Therefore, the excess air ratio of the IC engine can be accurately measured. The deviation between the measured and calculated values was within ±5%. Under each experimental condition, the in-cylinder pressure for 200 consecutive cycles was collected and analyzed using the Dewe-CA combustion analysis software. Then the profiles of the peak cylinder pressure, indicated thermal efficiency, coefficient of variation in indicated mean effective pressure (COVimep), etc versus excess air ratio were obtained by the software. Moreover, the engine combustion and emissions parameters for two syngas addition levels at lean conditions were compared and analyzed.

3. Results and discussion

3.1. *Effect of steam reforming*

The rates of hydrogen and carbon monoxide in the syngas directly reflect the quality of SRE in general. Fig. 2 displays the variations of hydrogen and carbon monoxide concentrations with excess air ratio at 1800 rpm and a MAP of 61.5 kPa. The syngas volume fraction reaches 2.5% in the intake gas when the feedstock flow rate reaches 40 mL/min. It can be found from Fig. 2 that the hydrogen concentration increases from 31.38% to 62.93% when the excess air ratio rises from 1.01 to 1.36. The proper reason for this can be ascribed to the fact that the reaction temperature is a key factor in the SRE. Although the in-cylinder temperature reduced with the increase of excess air ratio, the exhaust temperature is gradually raised due to the adversely improved post combustion. Therefore,

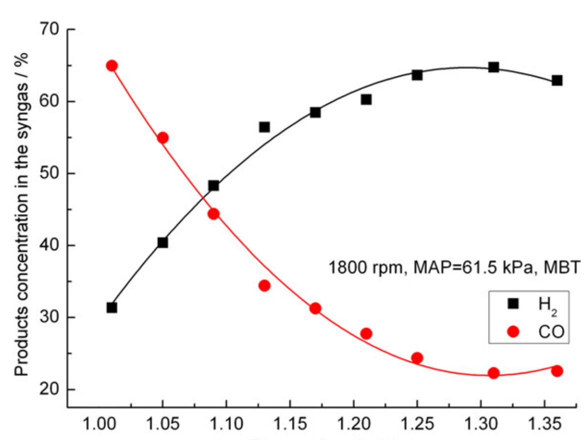

Fig. 2 – Products concentration in syngas versus excess air ratio at 2.5% syngas volume fraction.

the fuel reforming reactor could recover more exhaust heat when the engine is run at lean conditions.

Carbon monoxide is another important component in the syngas. Fig. 2 also indicates that carbon monoxide concentration decreases from 64.97% to 22.57% when the excess air ratio increases from 1.01 to 1.36. This is because carbon monoxide can further react according to the water gas shift reaction (WGSR) [33]. As a secondary reaction, the WGSR could consume more carbon monoxide and water steam to produce additional hydrogen.

3.2. Peak cylinder pressure and indicated thermal efficiency

The peak cylinder pressure (Pmax) represents the engine working capability to some extent. Fig. 3 depicts the variation of Pmax with excess air ratio at 1800 rpm and a MAP of 61.5 kPa. It can be seen from Fig. 3 that Pmax decreases with the increase of excess air ratio due to the reduced fuel energy flow rate at lean conditions. When the excess air ratio varies from 1.01 to 1.36, Pmax is decreased by 24.9% for the original engine and 18.4% for the 2.5% syngas-blended gasoline engine. Since the high flame and diffusion speeds of hydrogen and carbon monoxide enable the syngas-gasoline mixture to be burnt quickly and completely, Pmax is elevated with the increase of syngas addition fraction. Moreover, the low ignition energy of syngas also contributes to the enhancement in the peak cylinder pressure.

The engine indicated thermal efficiency is important for evaluating the engine fuel economy. The profiles of engine indicated thermal efficiency against excess air ratio at 1800 rpm and a MAP of 61.5 kPa are shown in Fig. 4. As it is seen from Fig. 4, the engine indicated thermal efficiency is increased with increase of excess air ratio for both the original and 2.5% syngas-blended gasoline engines. Moreover, for a specified excess air ratio, indicated thermal efficiency of the syngas-enriched engine is higher than that of the original one. When excess air ratio reaches 1.36, the peak indicated thermal efficiencies reach 38.6% and 40.0% for the original engine and the 2.5% syngas-blended gasoline engine. A possible interpretation could be attributed to the fact that the syngas-

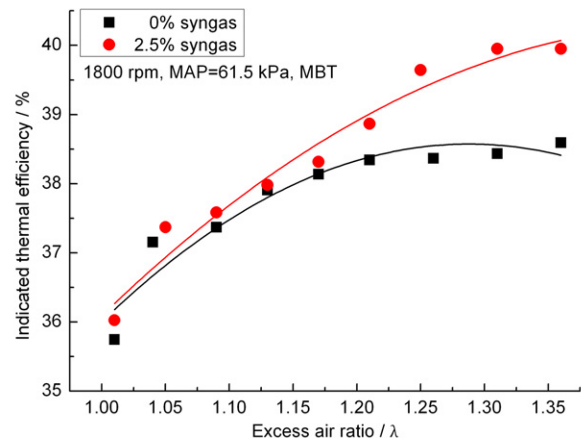

Fig. 4 – Indicated thermal efficiency versus excess air ratio at two syngas volume fractions of 0% and 2.5%.

gasoline mixture burns more completely than pure gasoline. Meanwhile, lean combustion has been proved to be an effective way for achieving higher engine thermal efficiency [34]. Furthermore, the short quenching distance of hydrogen also enables the flame of syngas–gasoline mixture to be propagated much closer to the cylinder wall and crevices.

3.3. Combustion analysis

Flame development (CA0-10) and propagation (CA10-90) periods are the main factors affecting the combustion quality. CA0-10 and CA10-90 are defined by the crank angle duration from spark discharge to 10% and from 10% to 90% heat release of the total fuel. Figs. 5 and 6 show the variations of CA0-10 and CA10-90 with excess air ratio at two syngas addition fractions of 0% and 2.5%, respectively. It can be found from Fig. 5 that CA0-10 is sharply prolonged from 26.1 to 41.4 °CA for the original engine when the excess air ratio increases from 1.01 to 1.36. At a specific excess air ratio, CA0-10 of the syngas-blended gasoline engine is shorter than that of original engine. Because the ignition energies of hydrogen and carbon

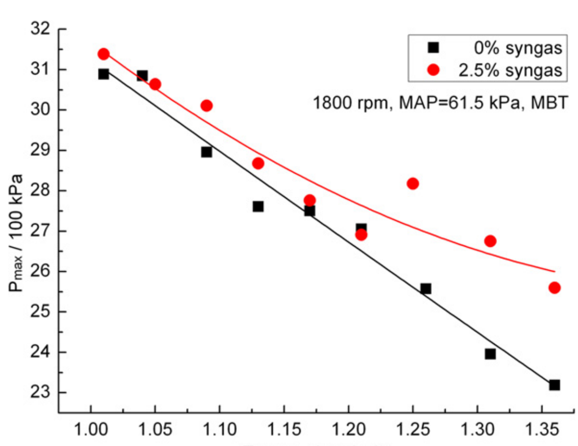

Fig. 3 – Peak cylinder pressure versus excess air ratio at two syngas volume fractions of 0% and 2.5%.

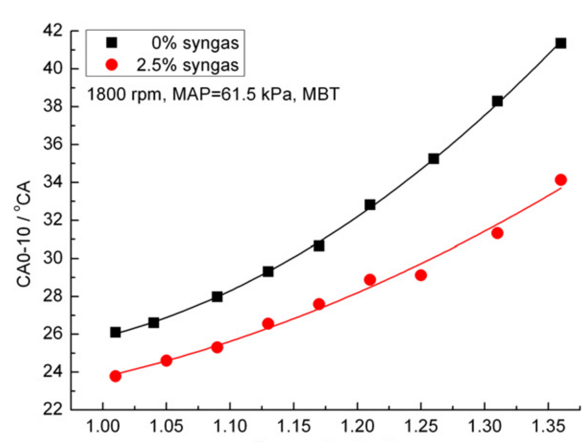

Fig. 5 – CA0-10 versus excess air ratio at two syngas volume fractions of 0% and 2.5%.

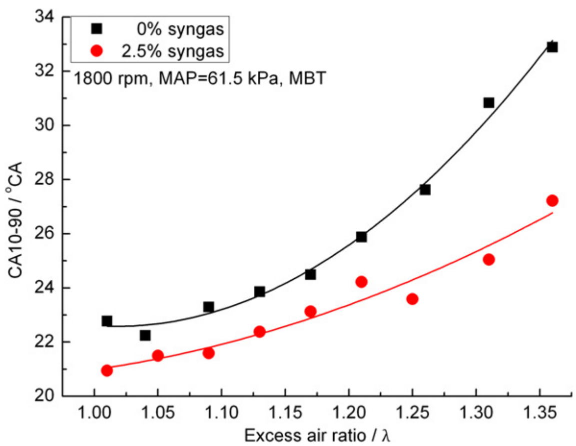

Fig. 6 – CA10-90 versus excess air ratio at two syngas volume fractions of 0% and 2.5%.

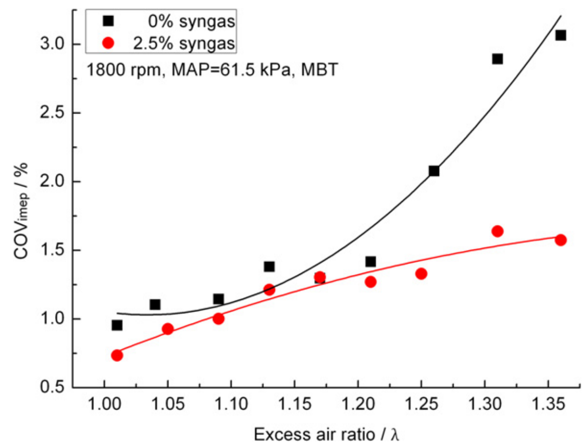

Fig. 7 – COVimep versus excess air ratio at two syngas volume fractions of 0% and 2.5%.

monoxide are lower than that of gasoline, the syngas can be ignited much more easily than the pure gasoline. Fig. 6 depicts that CA10-90 is also prolonged with the increase of excess air ratio due to the reduced burning speed at lean conditions. It can also be seen in Fig. 6 that the trend of variation of CA10-90 with excess air ratio at 2.5% syngas volume fraction is smoother than that of the original engine. A possible explanation is that the hydrogen and carbon monoxide in the syngas help stimulate the formation of O and OH radicals which improve the chain reaction in the fuel combustion process [35]. Moreover, since the hydrogen and carbon monoxide possess a higher burning speed than gasoline, the flame of syngas–gasoline mixture can be propagated more easily and quickly than that of pure gasoline. Therefore, both CA0-10 and CA10-90 are obviously shortened after the syngas blending.

3.4. Cyclic variation

The cyclic variation reflects engine lean operating ability, which influences the engine economical and dynamic performances [36,37]. The most representative parameter for evaluating the engine cyclic variation is the coefficient of variation in indicated mean effective pressure (COVimep). COVimep is defined as:

$$\text{COVimep} = \left[\sqrt{\sum_{i-1}^{k}\left(\text{imep}_i - \overline{\text{imep}}\right)^2/(k-1)}\Big/\overline{\text{imep}}\right] \times 100\% \qquad (3)$$

In Eq. (3) $\overline{\text{imep}} = (\sum_{i=1}^{k} \text{imep}_i)/k$ (kPa), where imep_i is the indicated mean effective pressure of the ith engine cycle (kPa), k is the number of engine consecutive cycles, and $\overline{\text{imep}}$ is the average value of the indicated mean effective pressure of k cycles (kPa).

The curves of COVimep against excess air ratio at two syngas volume fractions in the intake of 0% and 2.5% are plotted in Fig. 7. As it is shown in Fig. 7, COVimep of the engine fueled with pure gasoline increases sharply with the increase of excess air ratio. For the original engine, COVimep quickly increases from 1.0% to 3.1% when the excess air ratio increases from 1.01 to 1.36. Comparatively, COVimep of the 2.5% syngas-blended gasoline engine varies relatively smoothly with the increase of excess air ratio. Compared with the original engine, COVimep of the syngas-enriched gasoline engine shows a noticeable decrease, especially at high excess air ratios. It shows that the engine lean burn stability is effectively improved by the syngas addition. This is because the high diffusion speed of hydrogen in the syngas contributes to the enhanced charge homogeneity. Furthermore, the shortened CA0-10 and CA10-90 after the syngas addition also help ease the engine cyclic variation.

3.5. Emissions

HC, CO, and NOx are main toxic pollutants produced from the SI engines. In this section, the effect of syngas addition on emissions characteristics is discussed. Fig. 8 depicts the profiles of HC emissions against excess air ratio at 1800 rpm and a MAP of 61.5 kPa. Fig. 8 shows that, for a given syngas addition level, HC emissions are initially slightly reduced and then sharply increase with the increase of excess air ratio. The proper reason is that the gasoline flow rate is reduced with the

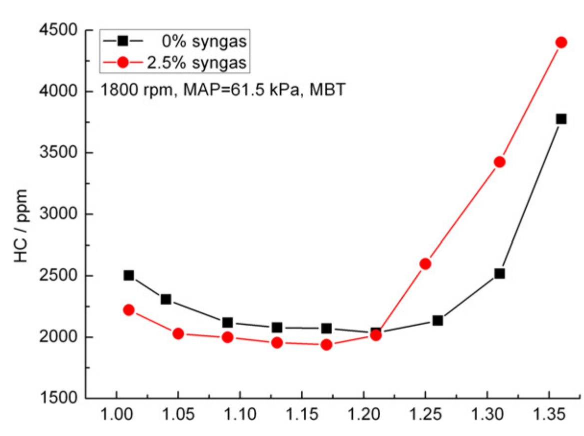

Fig. 8 – HC emissions versus excess air ratio at two syngas volume fractions of 0% and 2.5%.

increase of excess air ratio. Also, the properly raised oxygen concentration in the cylinder also avails the complete combustion of the fuel–air mixture. However, the further increased excess air ratio tends to cause the serious incomplete burning of the mixtures. The incomplete burning leads to adversely raised HC emissions at high excess air ratios. Meanwhile, the effect of syngas addition on HC emissions shows an opposite trend at $\lambda < 1.21$ and $\lambda > 1.21$. A proper explanation is that the quenching distances of hydrogen and carbon monoxide are much shorter than that of gasoline. Therefore, the flame of syngas–gasoline mixture could propagate much closer to the cylinder wall and crevices than that of the pure gasoline. Moreover, the high flame and diffusion speeds of hydrogen and carbon monoxide also contribute to the complete combustion in cylinder. But when excess air ratio is further increased from 1.21, HC emissions are raised again after syngas enrichment. Because the flame propagation period is shortened after the syngas addition, the dropped cylinder pressure is achieved at the exhaust valve opening, and then the raised residue gas fraction causes the increased HC emissions at high excess air ratios [25].

The profiles of CO emission against excess air ratio at two syngas addition fractions are shown in Fig. 9. It can be seen in Fig. 9 that CO emission drops sharply with the increase of excess air ratio for both the original engine and the syngas-blended gasoline engine. The reason is that the increased oxygen concentration improves the oxidation of CO at lean conditions. Moreover, Fig. 9 also shows that CO emission is adversely increased after the syngas addition, especially at the stoichiometric condition. At an excess air ratio of 1.01, CO emission is increased by 43.6% when the syngas volume fraction in the intake gas rises from 0% to 2.5%. The reason is that carbon monoxide in the syngas leads to the increased CO emission after the syngas addition. Meanwhile, as hydrogen has a higher stoichiometric air-to-fuel ratio and flame speed than those of gasoline, the fast combustion of hydrogen may consume more adjacent O_2, and therefore suppresses the oxidation of CO.

Fig. 10 displays NOx emissions versus excess air ratio at an engine speed of 1800 rpm and a MAP of 61.5 kPa. Fig. 10 shows that, for a given syngas addition level, NOx emissions are first increased and then decreased with the increase of excess air ratio. This is because NOx emissions are influenced by the combustion temperature and oxygen concentration. When the excess air ratio is slightly increased, the raised oxygen concentration in the cylinder causes the increased NOx emissions. However, when the engine is further leaned out, the cylinder temperature drops sharply due to the decreased fuel energy flow rate. Fig. 10 also shows that, for a specified excess air ratio, the 2.5% syngas-blended gasoline engine expels larger amounts of NOx emissions than the original engine. This is because the wide flammability of syngas contributes to the complete combustion of the fuel–air mixture and therefore elevates the cylinder temperature. Thus, NOx emissions are slightly increased with the syngas enrichment.

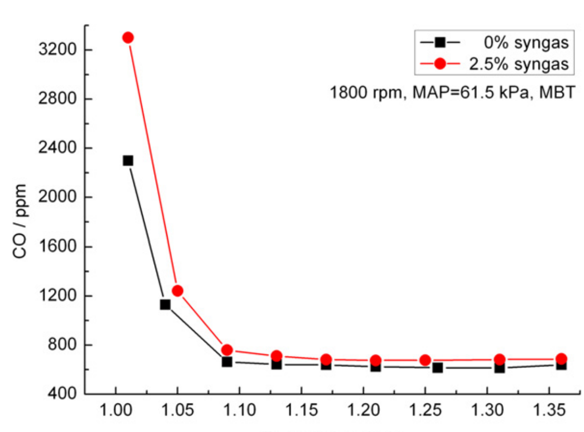

Fig. 9 – CO emission versus excess air ratio at two syngas volume fractions of 0% and 2.5%.

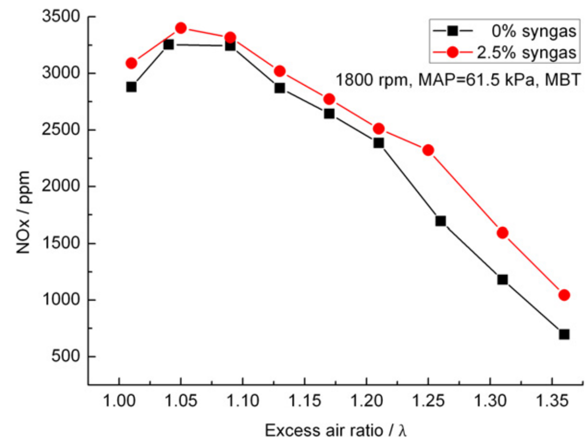

Fig. 10 – NOx emissions versus excess air ratio at two syngas volume fractions of 0% and 2.5%.

4. Summary

This paper investigated the effect of syngas addition on combustion and emissions performance of a gasoline engine at lean conditions. A self-designed fuel reforming reactor was applied to produce the syngas through recovering the engine exhaust heat. The engine was run at a constant 1800 rpm and a MAP of 61.5 kPa with two syngas volume fractions in the intake of 0% and 2.5%. The test results show that the hydrogen concentration in the syngas is increased with the increase of excess air ratio due to the increased exhaust gas temperature at lean conditions. Both the peak cylinder pressure and indicated thermal efficiency are enhanced with the increase of syngas addition. At an excess air ratio of 1.36, the engine indicated thermal efficiency is improved from 38.6% to 40.0% after syngas blending. Since hydrogen and carbon monoxide have much lower ignition energies and higher flame speeds than those of gasoline, both CA0-10 and CA10-90 are shortened after the syngas addition. COVimep is decreased after the syngas addition due to the shortened combustion period. At an excess air ratio of 1.36, COVimep reduces from 3.1% to 1.6% after syngas enrichment. CO and NOx emissions are slightly increased after the syngas addition. When the excess air ratio is smaller than 1.21, the syngas addition helps reduce

HC emissions. But, when the engine is further leaned out, the addition of syngas tends to cause increased HC emissions.

Acknowledgments

This work was supported by Key Program of Sci & Tech Project of Beijing Municipal Commission of Education (Grant No. KZ201210005002), Ph.D. Programs Foundation of Ministry of Education of China (Grant No. 20111103110010) and Beijing Municipal Natural Science Foundation (Grant No. 3122006).

Nomenclature

SRE	steam reforming of ethanol
MRG	methanol-reformed gas
DME	dimethyl ether
HCCI	homogeneous charge compression ignition
WGSR	water gas shift reaction
GC	gas chromatograph
OECU	original electronic control unit
HECU	hybrid electronic control unit
CA	crank angle
MAP	manifolds absolute pressure
α	syngas volume fraction in the total intake gas, %
λ	global excess air ratio
$\dot{v}_s$	volumetric flow rate of syngas, L/h
$\dot{v}_{air}$	volumetric flow rate of air, L/h
$\dot{m}_{air}$	mass flow rate of air, g/min
$\dot{m}_g$	mass flow rate of gasoline, g/min
$\dot{m}_{H_2}$	mass flow rate of hydrogen, g/min
$\dot{m}_{CO}$	mass flow rate of carbon monoxide, g/min
$AF_{st,g}$	stoichiometric air-to-fuel ratio of gasoline
AF_{st,H_2}	stoichiometric air-to-fuel ratio of hydrogen
$AF_{st,CO}$	stoichiometric air-to-fuel ratio of carbon monoxide
Pmax	peak cylinder pressure
COVimep	coefficient of variation in indicated mean effective pressure
CA0-10	CA duration of 0–10% heat release, °CA
CA10-90	CA duration of 10%–90% heat release, °CA

REFERENCES

[1] Dunn S. Hydrogen futures: toward a sustainable energy system. Int J Hydrogen Energy 2002;27:235–64.

[2] Huang Z, Liu B, Zeng K, Huang Y, Jiang D, Wang X, et al. Experimental study on engine performance and emissions for an engine fueled with natural gas-hydrogen mixtures. Energy Fuels 2006;20:2131–6.

[3] Salimi F, Shamekhi AH, Pourkhesalian AM. Role of mixture richness, spark and valve timing in hydrogen-fueled engine performance and emission. Int J Hydrogen Energy 2009;34:3922–9.

[4] Veziroglu TN, Barbir F. Hydrogen, the wonder fuel. Int J Hydrogen Energy 1992;17:391–404.

[5] Huang Z, Zhang Y, Wang Q, Wang J, Jiang D, Miao H. Study on flame propagation characteristics of natural gas-hydrogen-air mixtures. Energy Fuels 2006;20:2385–90.

[6] Huang Z, Wang J, Liu B, Zeng K, Yu J, Jiang D. Combustion characteristics of a direct-injection engine fueled with natural gas-hydrogen blends under various injection timings. Energy Fuels 2006;20:1498–504.

[7] Ji C, Wang S. Effect of hydrogen addition on the idle performance of a spark ignited gasoline engine at stoichiometric condition. Int J Hydrogen Energy 2009;34:3546–56.

[8] Huang Z, Wang J, Liu B, Zeng K, Yu J, Jiang D. Combustion characteristics of a direct-injection engine fueled with natural gas-hydrogen blends under different ignition timings. Fuel 2007;86:381–7.

[9] Boehman AL, Corre O. Combustion of syngas in internal combustion engines. Combust Sci Technol 2008;180:1193–206.

[10] Azimov U, Okuno M, Tsuboi K, Kawahara N, Tomita E. Multidimensional CFD simulation of syngas combustion in a micro-pilot-ignited dual-fuel engine using a constructed chemical kinetics mechanism. Int J Hydrogen Energy 2011;36:13793–807.

[11] Wang J, Chen H, Liu B, Huang Z. Study of cycle-by-cycle variations of a spark ignition engine fuelled with natural gas-hydrogen blends. Int J Hydrogen Energy 2008;33:4876–83.

[12] Huang Z, Zhang Y, Zeng K, Liu B, Wang Q, Jiang D. Measurements of laminar burning velocities for natural gas-hydrogen-air mixtures. Combust Flame 2006;146:302–11.

[13] Hu E, Huang Z, Liu B, Zheng J, Gu X. Experimental study on combustion characteristics of a spark-ignition engine fuelled with natural gas-hydrogen blends combining with EGR. Int J Hydrogen Energy 2009;34:1035–44.

[14] Zhang X, Huang Z, Zhang Z, Zheng J, Yu W, Jiang D. Measurements of laminar burning velocities and flame stability analysis for methanol-air-diluent mixtures at elevated temperatures and pressures. Int J Hydrogen Energy 2009;34:4862–75.

[15] Huang B, Hu E, Huang Z, Zheng J, Liu B, Jiang D. Cycle-by-cycle variations in a sparked ignition engine fueled with natural gas-hydrogen blends combined with EGR. Int J Hydrogen Energy 2009;34:8405–14.

[16] Ji C, Wang S. Experimental study on combustion and emissions performance of a spark ignition engine fueled with gasoline-hydrogen blends. Energy Fuels 2009;23:2930–6.

[17] Ganesh RH, Subramanian V, Balasubramanian V, Mallikarjuna JM, Ramesh A, Sharma RP. Hydrogen fueled spark ignition engine with electronically controlled manifold injection: an experimental study. Renew Energy 2008;33:1324–33.

[18] Ma F, Wang Y. Study on the extension of lean operation limit through hydrogen enrichment in a natural gas spark-ignition engine. Int J Hydrogen Energy 2008;33:1416–24.

[19] Ji C, Wang S. Combustion and emissions performance of a hybrid hydrogen-gasoline engine at idle and lean conditions. Int J Hydrogen Energy 2010;35:346–55.

[20] Al-Janabi HAKS, Al-Baghdadi MARS. A prediction study of the effect of hydrogen blending on the performance and pollutants emission of a four stroke spark ignition engine. Int J Hydrogen Energy 1999;24:363–75.

[21] Ji C, Wang S. Combustion and emissions characteristics of a hybrid hydrogen-gasoline engine under various loads and lean conditions. Int J Hydrogen Energy 2010;35:5714–22.

[22] Hu E, Huang Z, Liu B, Zheng J, Gu X, Huang B. Experimental investigation on performance and emissions of a spark-ignition engine fuelled with natural gas-hydrogen blends combined with EGR. Int J Hydrogen Energy 2009;34:528–39.

[23] Andrea TD, Henshaw PF, Ting DSK. The addition of hydrogen to a gasoline-fuelled SI engine. Int J Hydrogen Energy 2004;29:1541–52.

[24] Wang S, Ji C, Zhang B. Effect of hydrogen addition on combustion and emissions performance of a spark-ignited ethanol engine at idle and stoichiometric conditions. Int J Hydrogen Energy 2010;35:9205–13.
[25] Ji C, Wang S. Effect of hydrogen addition on combustion and emissions performance of a spark ignited gasoline engine at lean conditions. Int J Hydrogen Energy 2009;34:7823–34.
[26] Ji C, Wang S. Experimental study on combustion and emissions performance of a hybrid hydrogen-gasoline engine at lean burn limits. Int J Hydrogen Energy 2010;35: 1453–62.
[27] Shudo T. An HCCI combustion engine system using on-board reformed gases of methanol with waste heat recovery: ignition control by hydrogen. Int J Vehicle Des 2006;41: 206–26.
[28] Heracleous E. Well-to-wheels analysis of hydrogen production from bio-oil reforming for use in internal combustion engines. Int J Hydrogen Energy 2011;36: 11501–11.
[29] Raju ASK, Park CS, Norbeck JM. Synthesis gas production using steam hydrogasification and steam reforming. Fuel Process Technol 2009;90:330–6.
[30] Liguras DK, Kondarides DI, Verykios XE. Production of hydrogen for fuel cells by steam reforming of ethanol over supported noble metal catalysts. Appl Catal B 2003;43: 345–54.
[31] Profeti LPR, Ticianelli EA, Assaf EM. Ethanol steam reforming for production of hydrogen on magnesium aluminate-supported cobalt catalysts promoted by noble metals. Appl Catal A 2009;360:17–25.
[32] Park C, Choi Y, Kim C, Oh S, Lim G, Moriyoshi Y. Performance and exhaust emission characteristics of a spark ignition engine using ethanol and ethanol-reformed gas. Fuel 2010; 89:2118–25.
[33] Profeti LPR, Dias JAC, Assaf JM, Assaf EM. Hydrogen production by steam reforming of ethanol over Ni-based catalysts promoted with noble metals. J Power Sources 2009; 190:525–33.
[34] Rankin DD. Lean combustion technology and control. Elsevier; 2008. p. 1.
[35] Conte E, Boulouchos K. Influence of hydrogen-rich-gas addition on combustion, pollutant formation and efficiency of an IC-SI engine. In: SAE paper No.2004-01-0972; 2004.
[36] Heywood JB. Internal combustion engine fundamentals. New York: McGraw-Hill; 1988. p. 413–426.
[37] Lyon D. Knock and cyclic dispersion in a spark ignition engine, petroleum based fuels and automotive applications. In: I Mech E Conf Proc. London: MEP; 1986.